

## APPENDIX C

### Abbreviations, Constants and Symbols

#### C.1 Physical Constants

c	speed of light in vacuum, $c = 2.99792458 \cdot 10^8$ m/s
$\mu_0$	magnetic field constant, $\mu_0 = 4\pi \cdot 10^{-7} \frac{\text{N}}{\text{A}^2} = 1.2566370614 \cdot 10^{-6} \frac{\text{Vs}}{\text{Am}}$
$\epsilon_0$	dielectric constant of vacuum, $\epsilon_0 = \frac{1}{\mu_0 c^2} = 8.854187817 \cdot 10^{-12} \frac{\text{As}}{\text{Vm}}$
h	Planck constant, $h = 6.6260755 \cdot 10^{-34}$ Js; $\hbar = h/2\pi = 1.05457266 \cdot 10^{-34}$ Js
e	elementary charge, $e = 1.60217733 \cdot 10^{-19}$ C
$m_e$	electron mass, $m_e = 9.1093897 \cdot 10^{-31}$ kg
$m_p$	proton mass, $m_p = 1.6726231 \cdot 10^{-27}$ kg
$N_A$	Avogadro constant, $N_A = 6.0221367 \cdot 10^{23} \frac{1}{\text{mol}}$
F	Faraday constant, $F = N_A e = 96485.309 \frac{\text{C}}{\text{mol}}$
R	molar gas constant, $R = N_A k_B = 8.314510 \frac{\text{J}}{\text{molK}}$
$k_B$	Boltzmann's constant, $k_B = R/N_A = 1.380658 \cdot 10^{-23} \frac{\text{J}}{\text{K}}$
electron volt, $eV = (e/C) J = \{e\} J = 1.60217733 \cdot 10^{-19}$ J	
(unified) atomic mass unit, $1u = m_u = 1/12 m(^{12}\text{C}) = 1.6605402 \cdot 10^{-27}$ kg	

## C.2 Abbreviations used in the text

ADP	adenosine-diphosphate;
<i>A. nidulans</i>	<i>Anacystis nidulans</i> ;
ATP	adenosine-triphosphate;
bis-Cc	cytochrome c with bis-histidine ligated heme;
Cb	cytochrome b;
Cbc <sub>1</sub>	cytochrome bc <sub>1</sub> ;
Cb <sub>6f</sub>	cytochrome b <sub>6f</sub> ;
CcPo	cytochrome c peroxidase;
CPD	cyclobutan-pyrimidin dimer;
CPU	central processing unit;
Cyt	cytochrome;
DNA	deoxyribonucleotide acid;
DPA	diphosphoric acid;
<i>E. coli</i>	<i>Escherichia coli</i> ;
ET	electron transfer;
FAD	flavin-adeninucleotide;
Hb	hemoglobin;
H <sub>h</sub>	high potential heme;
H <sub>l</sub>	low potential heme;
ISP	iron-sulfur protein (Rieske protein);
LPBE	linearized Poisson-Boltzmann equation;
Mb	myoglobin;
MC	Monte Carlo;
MD	molecular dynamics;
mono-Cc	cytochrome c with mono-histidine ligated heme;
MTHF	5,10-methenyltetrahydrofolat, folic acid;
NAD	nicotinamide adenine dinucleotide;
PBE	Poisson-Boltzmann equation;
PDB	Protein Data Bank;
PR	propionic acid;
PRA	propionic acid at pyrrole ring A;
PRD	propionic acid at pyrrole ring D;
RMS	root-mean-square;

### C.3 Formula Symbols

$\beta$	$\beta = 1/k_B T$ ;
$c_s^{\text{bulk}}(\vec{r})$	concentration of an ion $s$ at $\vec{r}$ ;
$D$	the closest distance between the electron donor and acceptor;
$\epsilon$	dielectric constant, a value of $\epsilon_p = 4$ is used for the protein and $\epsilon_s = 80$ is used for the solvent;
$\Delta G$	Gibb' s energy, free energy;
$\Delta\Delta G_{\mu}^{\text{back}}$	background energy term (defined in equation 2.36);
$\Delta\Delta G_{\mu}^{\text{Born}}$	Born energy term (defined in equation 2.35);
$G_{\mu}$	thermodynamic average energy (defined in equation 2.49);
$G^n$	protonation state energy (defined in equation 2.40);
$I(\vec{r})$	ionic strength $I(\vec{r}) = \frac{1}{2} \sum_s c_s^{\text{bulk}}(\vec{r}) q_s^2$ ;
$k_B$	Boltzmann constant;
$k^{\text{ET}}$	reaction rate of electron transfer reaction (see eqs. 7.1 and 7.2);
$k^{\text{PT}}$	reaction rate of protonation reaction (see equation 7.3);
$\kappa$	inverse Debye length $\kappa^2(\vec{r}) = 8\pi\beta I(\vec{r})$ ;
$l$	grid constant of the cubic lattice used to solve the LPBE;
$\lambda$	reorganization energy of the ET process;
$\ln$	natural logarithm;
$\log$	decadic logarithm;
$\nabla$	gradient operator $\nabla = (\frac{\partial}{\partial x} + \frac{\partial}{\partial y} + \frac{\partial}{\partial z})$ ;
$\nabla^2$	Laplace operator $\nabla^2 = (\frac{\partial}{\partial x^2} + \frac{\partial}{\partial y^2} + \frac{\partial}{\partial z^2})$ ;
$\text{pH}$	negative decadic logarithm of the hydrogen ion concentration (defined in equation 2.5);
$\phi(\vec{r})$	electrostatic potential at the position $\vec{r}$ (defined in eq. 2.21);
$\text{pK}_a$	negative decadic logarithm of the equilibrium constant of a deprotonation reaction (defined in equation 2.6);
$\text{pK}_{a,\mu}^{\text{intr}}$	intrinsic $\text{pK}_a$ value (defined in equation 2.37);
$q_i$	charge of an ion $i$ ;
$\vec{r}$	coordinates of a point in three-dimensional space;
$\rho(\vec{r})$	charge distribution (density) at the position $\vec{r}$ ;
$T$	absolute temperature in Kelvin ( $273.15 \text{ K} = 0^\circ\text{C}$ );
$W_{\mu\nu}$	element of the $W$ matrix (defined in equation 2.39);
$\vec{x}^n$	$N$ -dimensional protonation state vector;
$x_{\mu}^n$	element of the $\vec{x}^n$ vector, that shows the protonation state of the group $\mu$ in the protonation state $n$ of the protein;
$\langle x_{\mu} \rangle$	protonation probability (defined in equation 2.9 for acid in aqueous solution, and in equation 2.48 for a protein).

## APPENDIX D

The pK<sub>a</sub> and E<sup>0</sup> values of the model compounds**Table D1.** Groups considered as titratable with the pK<sub>a</sub> values of their model compounds and redox potentials E<sup>0</sup> of some redox-active compounds

titratable group	model compound pK <sub>a</sub>	reference
arginine	12.0	Nozaki & Tanford (1967)
aspartate	4.0	Nozaki & Tanford (1967)
cystein	9.5	Nozaki & Tanford (1967)
glutamate	4.4	Nozaki & Tanford (1967)
δ-histidine	7.0	Tanokura (1983)
ε-histidine	6.6	Tanokura (1983)
lysine	10.4	Nozaki & Tanford (1967)
tyrosine (YH/Y <sup>-</sup> )	9.6	Nozaki & Tanford (1967)
tyrosine (YH <sup>+</sup> •/Y•)	-2.0	Dixon & Murphy (1976)
C-terminus	3.8	Nozaki & Tanford (1967)
N-terminus	7.5	Nozaki & Tanford (1967)
heme propionate	4.8	Moore & Pettigrew (1990)
tryptophan (WH/W <sup>-</sup> )	16.82	Yagil (1967)
tryptophan (WH <sup>+</sup> •/W•)	4.0	Solar (1991)
phosphate pK <sub>a,1</sub>	1.96	Holleman & Wiberg (1964)
phosphate pK <sub>a,2</sub>	6.92	Holleman & Wiberg (1964)
phosphate pK <sub>a,3</sub>	11.72	Holleman & Wiberg (1964)
diphosphate pK <sub>a,1</sub>	0.85	taken from handbook Stryer (1988)
diphosphate pK <sub>a,2</sub>	1.49	taken from handbook Stryer (1988)
diphosphate pK <sub>a,3</sub>	5.77	taken from handbook Stryer (1988)
diphosphate pK <sub>a,4</sub>	8.22	taken from handbook Stryer (1988)
water pK <sub>a,1</sub>	-1.7	Weast (1986)
water pK <sub>a,2</sub>	15.7	Weast (1986)

redox couple	model compound E <sup>0</sup> (mV)	reference
heme model (met, his)	-70	Wilson (1983)
heme model (his, his)	-220	Wilson (1983)
tryptophan (WH <sup>+</sup> •/WH)	+1070	Dutton (1999)
tyrosine (YH <sup>+</sup> •/YH)	+1376	extrapolated from Solar (1991)
flavin: FADH <sup>+</sup> •/FADH <sup>-</sup>	-290	Wardman (1989)

## APPENDIX E

Table E1. Atomic partial charges of titratable groups

arginine		
atom	protonated	deprotonated
N- $\epsilon$	-0.70	-0.81
H- $\epsilon$	0.44	0.44
C- $\zeta$	0.64	0.71
N- $\eta_1$	-0.80	-0.90
H- $\eta_{11}$	0.46	0.27
H- $\eta_{12}$	0.46	0.27
N- $\eta_2$	-0.80	-0.90
H- $\eta_{21}$	0.46	0.27
N- $\eta_{22}$	0.46	0.27

$\delta$ -histidine		
atom	protonated	deprotonated
N- $\epsilon_2$	-0.51	-0.70
C- $\gamma$	0.19	-0.05
N- $\delta_1$	-0.51	-0.36
H- $\delta_1$	0.44	0.32
C- $\epsilon_1$	0.32	0.25
H- $\epsilon_2$	0.44	0.00
C- $\delta_2$	0.19	0.22
C- $\beta$	-0.05	-0.09
H- $\delta_2$	0.13	0.10
H- $\epsilon_1$	0.18	0.13

$\epsilon$ -histidine		
atom	protonated	deprotonated
N- $\epsilon_2$	-0.51	-0.36
C- $\gamma$	0.19	0.22
N- $\delta_1$	-0.51	-0.70
H- $\delta_1$	0.44	0.00
C- $\epsilon_1$	0.32	0.25
H- $\epsilon_2$	0.44	0.32
C- $\delta_2$	0.19	-0.05
C- $\beta$	-0.05	-0.08
H- $\delta_2$	0.13	0.09
H- $\epsilon_1$	0.18	0.13

N-terminus		
atom	protonated	deprotonated
NT	-0.30	-0.97
HT1	0.33	0.22
HT2	0.33	0.22
HT3	0.33	0.22

lysine		
atom	protonated	deprotonated
N- $\zeta$	-0.30	-0.97
H- $\zeta_1$	0.33	0.22
H- $\zeta_2$	0.33	0.22
H- $\zeta_3$	0.33	0.22

cysteine		
atom	protonated	deprotonated
C- $\beta$	-0.11	-0.25
S- $\gamma$	-0.23	-0.93
H- $\gamma$	0.16	0.00

glutamate		
atom	protonated	deprotonated
C- $\gamma$	-0.21	-0.28
C- $\delta$	0.75	0.62
O- $\epsilon_1$	-0.36	-0.76
O- $\epsilon_2$	-0.36	-0.76

aspartate		
atom	protonated	deprotonated
C- $\beta$	-0.21	-0.28
C- $\gamma$	0.75	0.62
O- $\delta_1$	-0.36	-0.76
O- $\delta_2$	-0.36	-0.76

tyrosine		
atom	protonated	deprotonated
C- $\zeta$	0.11	-0.18
O- $\eta$	-0.54	-0.82
H- $\eta$	0.43	0.00

C-terminus		
atom	protonated	deprotonated
CT	0.34	0.34
OT1	-0.17	-0.67
OT2	-0.17	-0.67

heme propionate		
atom	protonated	deprotonated
C- $\beta$	-0.21	-0.28
C- $\gamma$	0.75	0.62
O1	-0.36	-0.76
O2	-0.36	-0.76

**Table E2.** Atomic partial charges for the bis-imidazole heme model compounds of artificial and native cytochrome b

atom	charges of hemes with axial imidazoles							
	artificial cyt b				native cyt b			
	Hl		Hh		Hl		Hh	
	oxd	red	oxd	red	oxd	red	oxd	red
<b>FE</b>	0.480	0.250	0.480	0.250	0.480	0.250	0.480	0.250
<b>NA</b>	-0.182	-0.187	-0.082	-0.113	-0.114	-0.102	-0.390	-0.401
<b>NB</b>	-0.079	-0.060	-0.008	-0.040	-0.033	-0.050	-0.311	-0.289
<b>NC</b>	-0.083	-0.054	-0.101	-0.091	-0.064	-0.056	-0.110	-0.040
<b>ND</b>	-0.159	-0.116	-0.064	-0.096	-0.310	-0.316	-0.169	-0.121
<b>C1A</b>	-0.040	-0.015	-0.058	-0.050	-0.101	-0.098	0.119	0.048
<b>C2A</b>	0.195	0.068	0.221	0.192	0.285	0.187	0.021	0.042
<b>C3A</b>	-0.042	-0.016	-0.032	0.004	-0.059	-0.047	0.100	0.052
<b>C4A</b>	-0.067	-0.102	-0.008	-0.049	-0.011	-0.014	0.003	0.093
<b>C1B</b>	-0.028	-0.059	0.076	-0.012	-0.023	-0.035	-0.030	0.004
<b>C2B</b>	0.038	0.028	0.057	0.015	0.029	0.006	0.248	0.210
<b>C3B</b>	0.020	-0.005	0.021	-0.027	0.016	-0.006	-0.119	-0.101
<b>C4B</b>	-0.046	-0.066	0.009	-0.031	-0.007	-0.039	0.251	0.110
<b>C1C</b>	-0.019	-0.038	0.008	-0.011	-0.019	-0.041	-0.058	-0.172
<b>C2C</b>	0.036	-0.003	0.104	0.081	0.054	0.042	0.238	0.231
<b>C3C</b>	-0.001	-0.024	0.127	0.010	0.011	0.007	0.170	-0.211
<b>C4C</b>	-0.033	-0.091	-0.042	-0.066	-0.053	0.063	0.071	0.033
<b>C1D</b>	-0.006	-0.033	0.046	-0.001	0.005	-0.012	-0.010	0.000
<b>C2D</b>	-0.054	-0.028	-0.189	-0.192	-0.012	0.003	0.098	0.052
<b>C3D</b>	0.261	0.146	0.242	0.203	0.384	0.245	0.139	0.149
<b>C4D</b>	-0.071	-0.053	-0.016	-0.164	-0.235	-0.198	-0.049	-0.120
<b>CHA</b>	0.001	-0.005	-0.023	-0.138	0.036	0.028	-0.171	-0.109
<b>HA</b>	0.119	0.077	0.133	0.109	0.095	0.068	0.111	0.098
<b>CHB</b>	-0.002	-0.018	-0.001	-0.082	-0.092	-0.162	-0.039	-0.161
<b>HB</b>	0.063	0.055	0.044	0.043	0.099	0.099	0.101	0.100
<b>CHC</b>	-0.048	-0.087	-0.083	-0.170	-0.044	-0.053	-0.219	-0.121
<b>HC</b>	0.074	0.052	0.083	0.058	0.077	0.072	0.120	0.090
<b>CHD</b>	-0.025	-0.054	-0.028	-0.050	-0.004	-0.043	-0.148	-0.171
<b>HD</b>	0.085	0.073	0.099	0.055	0.083	0.059	0.102	0.091
<b>CMA</b>	-0.152	-0.130	-0.337	-0.271	-0.287	-0.250	-0.391	-0.389
<b>1HMA</b>	0.060	0.043	0.116	0.084	0.092	0.070	0.120	0.103
<b>2HMA</b>	0.060	0.043	0.116	0.084	0.092	0.070	0.120	0.110
<b>3HMA</b>	0.060	0.043	0.116	0.084	0.092	0.070	0.090	0.090
<b>CAA</b>	-0.280	-0.280	-0.280	-0.280	-0.270	-0.270	-0.270	-0.270
<b>HAA1</b>	0.090	0.090	0.090	0.090	0.090	0.090	0.090	0.090
<b>HAA2</b>	0.090	0.090	0.090	0.090	0.090	0.090	0.090	0.090
<b>CMB</b>	-0.151	-0.131	-0.230	-0.231	-0.183	-0.185	-0.459	-0.449
<b>1HMB</b>	0.059	0.045	0.078	0.064	0.063	0.051	0.110	0.100
<b>2HMB</b>	0.059	0.045	0.078	0.064	0.063	0.051	0.140	0.120

<b>3HMB</b>	0.059	0.045	0.078	0.064	0.063	0.051	0.140	0.120
<b>CAB</b>	-0.051	-0.043	-0.075	-0.071	-0.112	-0.099	-0.062	-0.042
<b>HAB</b>	0.066	0.060	0.075	0.064	0.101	0.086	0.080	0.070
<b>CBB</b>	-0.185	-0.218	-0.163	-0.233	-0.127	-0.149	-0.180	-0.210
<b>1HBB</b>	0.093	0.077	0.094	0.070	0.067	0.056	0.090	0.090
<b>2HBB</b>	0.093	0.077	0.094	0.070	0.067	0.056	0.090	0.072
<b>CMC</b>	-0.149	-0.130	-0.209	-0.193	-0.161	-0.172	-0.398	-0.389
<b>1HMC</b>	0.062	0.044	0.074	0.060	0.060	0.057	0.110	0.099
<b>2HMC</b>	0.062	0.044	0.074	0.060	0.060	0.057	0.090	0.079
<b>3HMC</b>	0.062	0.044	0.074	0.060	0.060	0.057	0.140	0.120
<b>CAC</b>	-0.038	-0.034	-0.070	-0.076	-0.081	-0.081	0.000	0.030
<b>HAC</b>	0.052	0.050	0.070	0.070	0.074	0.073	0.058	0.049
<b>CBC</b>	-0.162	-0.187	-0.149	-0.167	-0.153	-0.178	-0.199	-0.240
<b>1HBC</b>	0.083	0.066	0.087	0.073	0.084	0.071	0.098	0.098
<b>2HBC</b>	0.083	0.066	0.087	0.073	0.084	0.071	0.072	0.060
<b>CMD</b>	-0.169	-0.133	-0.198	-0.188	-0.448	-0.404	-0.392	-0.382
<b>1HMD</b>	0.062	0.043	0.090	0.063	0.137	0.112	0.110	0.101
<b>2HMD</b>	0.062	0.043	0.090	0.063	0.137	0.112	0.130	0.110
<b>3HMD</b>	0.062	0.043	0.090	0.063	0.137	0.112	0.120	0.102
<b>CAD</b>	-0.280	-0.280	-0.280	-0.280	-0.270	-0.270	-0.260	-0.260
<b>HAD1</b>	0.090	0.090	0.090	0.090	0.090	0.090	0.090	0.090
<b>HAD2</b>	0.090	0.090	0.090	0.090	0.090	0.090	0.090	0.090
<b>1ND1</b>	-0.237	-0.240	-0.295	-0.216	-0.109	-0.105	-0.250	-0.270
<b>1HD1</b>	0.133	0.122	0.234	0.287	0.266	0.249	0.318	0.298
<b>1CG</b>	0.097	0.053	-0.084	0.003	0.004	-0.044	-0.031	-0.051
<b>1CB</b>	-0.090	-0.090	-0.090	-0.090	-0.090	-0.090	-0.050	-0.070
<b>1HB1</b>	0.090	0.090	0.090	0.090	0.090	0.090	0.090	0.090
<b>1HB2</b>	0.090	0.090	0.090	0.090	0.090	0.090	0.090	0.090
<b>1NE2</b>	0.024	0.054	-0.199	-0.010	0.025	0.054	0.210	0.210
<b>1CD2</b>	-0.096	-0.087	-0.044	-0.049	-0.139	-0.136	-0.100	-0.100
<b>1HD2</b>	0.050	0.053	0.008	0.069	0.170	0.169	0.089	0.081
<b>1CE1</b>	0.207	0.260	-0.005	0.141	-0.013	0.003	0.041	0.019
<b>1HE1</b>	0.079	0.060	0.025	0.084	0.108	0.109	0.141	0.129
<b>2ND1</b>	-0.208	-0.213	-0.107	-0.105	-0.245	-0.235	-0.160	-0.170
<b>2HD1</b>	0.203	0.193	0.285	0.266	0.310	0.290	0.308	0.289
<b>2CG</b>	0.025	-0.016	-0.012	-0.068	0.023	-0.021	-0.072	-0.111
<b>2CB</b>	-0.090	-0.090	-0.090	-0.090	-0.090	-0.090	-0.030	-0.040
<b>2HB1</b>	0.090	0.090	0.090	0.090	0.090	0.090	0.090	0.090
<b>2HB2</b>	0.090	0.090	0.090	0.090	0.090	0.090	0.090	0.090
<b>2NE2</b>	0.004	0.030	-0.026	0.017	-0.066	-0.068	0.288	0.309
<b>2CD2</b>	-0.084	-0.059	-0.054	-0.034	-0.001	0.019	-0.151	-0.151
<b>2HD2</b>	0.071	0.065	0.111	0.102	0.064	0.058	0.122	0.110
<b>2CE1</b>	0.172	0.181	-0.029	0.006	0.018	0.026	-0.039	0.070
<b>2HE1</b>	0.051	0.059	0.047	0.077	0.131	0.136	0.140	0.140

**Table E3.** Atomic partial charges of some cofactors and special titratable groups used in photolyase

folic acid - MF1		
atom	Protonated	deprotonated
C23	0.743	0.743
O24	-0.301	-0.801
O25	-0.301	-0.801

folic acid - MF2		
atom	Protonated	deprotonated
C27	-0.107	-0.291
C28	0.900	0.884
O29	-0.462	-0.862
O30	-0.462	-0.862

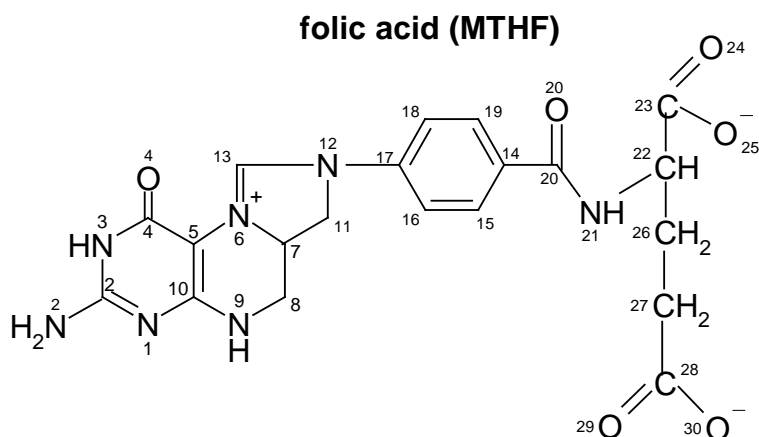
  

folic acid	
atom	charge
N1	-0.849
C2	1.217
N2	-1.263
H2a	0.482
H2b	0.531
N3	-0.854
H3	0.464
C4	0.853
O4	-0.622
C5	-0.657
N6	0.105
C7	0.131
H7	0.055
C8	0.137
H8a	0.065
H8b	0.090
N9	-0.747
H9	0.431
C10	0.786
C11	-0.009
H11a	0.122
H11b	0.047
N12	-0.265
C13	0.296
H13	0.193
C14	-0.068
C15	-0.034
H15	0.143

folic acid	
atom	charge
C16	-0.302
H16	0.198
C17	0.159
C18	-0.319
H18	0.201
C19	-0.030
H19	0.164
C20	0.722
O20	-0.629
N21	-0.780
H21	0.367
C22	0.185
H22	0.031
C23	0.743
O24	-0.801
O25	-0.801
C26	0.232
H26a	-0.060
H26a	-0.060
C27	-0.291
H27a	0.012
H27b	0.074
C28	0.884
O29	-0.862
O30	-0.862

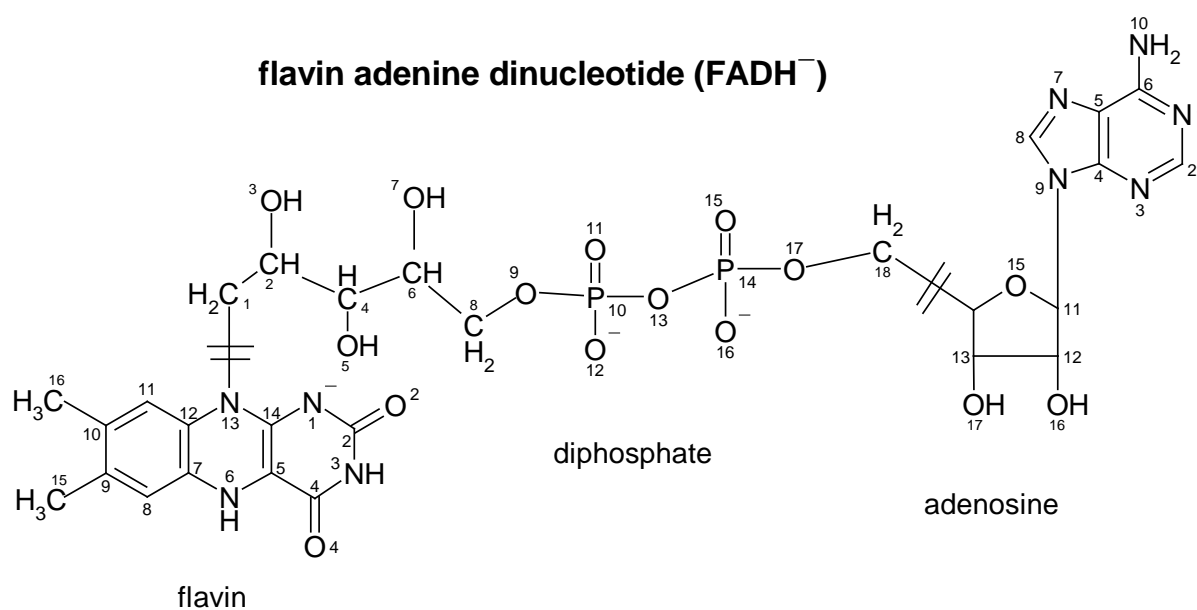
Atom numbers refer to the displayed bond topologies of the folic acid and the components of FADH: adenosine, flavin and diphosphoric acid. Hydrogen atoms are labeled according to the atom number of the atom to which they are bound. Several hydrogen atoms bound to the same atom are discriminated by lower case letters (a, b,c).



flavin	
atom	charge
N1	-0.926
C2	1.019
O2	-0.743
N3	-0.843
H3	0.382
C4	0.929
O4	-0.740
C5	-0.607
N6	-0.345
H6	0.297
C7	0.170
C8	-0.520
H8	0.251
C9	0.048
C10	0.151
C11	-0.627
H11	0.327
C12	0.383
N13	-0.557
C14	0.705
C15	-0.185
H15a	0.059
H15b	0.058
H15c	0.041
C16	-0.345
H16a	0.096
H16b	0.095
H16c	0.099

diphosphate group	
atom	charge
C1	0.460
H1a	-0.027
H1b	-0.047
C2	0.238
H2	-0.096
O3	-0.743
H3	0.401
C4	0.978
H4	-0.204
O5	-0.740
H5	0.323
C6	0.012
H6	-0.024
O7	-0.735
H7	0.399
C8	0.758
H8a	-0.152
H8b	-0.081
O9	-0.715
P10	1.513
O11	-0.442
O12	-0.442
O13	-0.456
P14	1.431
O15	-0.421
O16	-0.421
O17	-0.385
C18	-0.218
H18a	0.105
H18b	0.096

adenosine	
atom	charge
N1	-0.922
C2	0.650
H2	0.044
N3	-0.839
C4	0.604
C5	-0.146
C6	0.988
N7	-0.668
C8	0.512
H8	0.104
N9	-0.428
N10	-1.202
H10a	0.428
H10b	0.477
C11	0.577
H11	0.014
C12	-0.012
H12	0.132
C13	0.918
H13	-0.368
C14	0.466
H14	-0.038
O15	-0.633
O16	-0.775
H16	0.460
O17	-0.912
H17	0.532



flavin (variable charges)		
atom	FADH <sup>•</sup>	FADH <sup>-</sup>
N1	-0.705	-0.926
C2	0.938	1.019
O2	-0.603	-0.743
N3	-0.829	-0.843
H3	0.408	0.382
C4	0.817	0.929
O4	-0.653	-0.740
C5	-0.360	-0.607
N6	-0.225	-0.345
H6	0.425	0.297
C7	0.120	0.170
C8	-0.361	-0.520
H8	0.196	0.251
C9	0.068	0.048
C10	0.168	0.151
C11	-0.490	-0.627
H11	0.271	0.327
C12	0.322	0.383
N13	-0.437	-0.557
C14	0.684	0.705
C15	-0.185	-0.185
H15a	0.059	0.059
H15b	0.058	0.058
H15c	0.041	0.041
C16	-0.345	-0.345
H16a	0.096	0.096
H16b	0.095	0.095
H16c	0.099	0.099

diphosphate group (variable charges)			
atom	protonated	deprot. at P10	deprot. at P14
O9	-0.715	-0.715	-0.715
P10	1.513	1.353	1.513
O11	-0.442	-0.862	-0.442
O12	-0.442	-0.862	-0.442
O13	-0.456	-0.456	-0.456
P14	1.431	1.431	1.271
O15	-0.421	-0.421	-0.841
O16	-0.421	-0.421	-0.841
O17	-0.385	-0.385	-0.385

tryptophan			
atom	WH <sup>•</sup>	WH	W <sup>•</sup>
C-β	-0.348	-0.359	-0.374
H-β <sub>1</sub>	0.249	0.187	0.202
H-β <sub>2</sub>	0.249	0.187	0.202
C-γ	-0.018	-0.059	-0.031
C-δ <sub>1</sub>	0.297	0.042	0.057
H-δ <sub>1</sub>	0.319	0.270	0.204
N-ε <sub>1</sub>	-0.780	-0.851	-0.488
H-ε <sub>1</sub>	0.453	0.393	0.000
C-ε <sub>2</sub>	0.316	0.324	0.205
C-δ <sub>2</sub>	-0.027	-0.054	0.013
C-ε <sub>3</sub>	-0.163	-0.206	-0.183
H-ε <sub>3</sub>	0.254	0.194	0.204
C-ζ <sub>3</sub>	-0.203	-0.223	-0.210
H-ζ <sub>3</sub>	0.254	0.194	0.204
C-ζ <sub>2</sub>	-0.182	-0.216	-0.215
H-ζ <sub>2</sub>	0.264	0.194	0.205
C-η <sub>2</sub>	-0.191	-0.211	-0.199
H-η <sub>2</sub>	0.257	0.194	0.204

tyrosine			
atom	YH <sup>•</sup>	YH	Y <sup>•</sup>
Cβ	-0.180	-0.180	-0.180
H-β <sub>1</sub>	0.090	0.090	0.090
H-β <sub>2</sub>	0.090	0.090	0.090
C-γ	0.428	0.156	0.189
C-δ <sub>1</sub>	-0.230	-0.261	-0.245
H-δ <sub>1</sub>	0.223	0.177	0.163
C-ε <sub>1</sub>	-0.230	-0.261	-0.245
H-ε <sub>1</sub>	0.223	0.177	0.163
C-ζ	0.621	0.351	0.494
O-η	-0.430	-0.542	-0.355
H-η	0.409	0.371	0.000
C-δ <sub>2</sub>	-0.230	-0.261	-0.245
H-δ <sub>2</sub>	0.223	0.177	0.163
C-ε <sub>2</sub>	-0.230	-0.261	-0.245
H-ε <sub>2</sub>	0.223	0.177	0.163





## APPENDIX G

### Comparison the amino acid sequences of four-helix bundles for native Cb, artificial Cb and Maquette

The amino acids of the two heme-binding helices *B* and *D* and that of the two shielding helices *A* and *C* have been adapted to design the hydrophobic face of helix *F* and *G*, respectively, in the artificial Cb. For comparison, the sequences of the helices *A*, *B*, *C* and *D* from *Rhodobacter captulatus* with the conserved residues marked in bold are shown in addition to the sequence of the *Maquette* designed by Robertson et al.

N-terminus (at template of Cb)

C-terminus (at open end of Cb)

helix *F*<sup>1</sup>:

1 2 3 4 5 6 7 8 9 0 1 2 3 4 5 6 7 8 9 0 1 2 3 4 5 6 7 8 9  
BrAc G G E L **R** E L **H** E K L A K Q **F** E Q L V K L **H** E E **R** A K K L NH<sub>2</sub>

helix *B*<sup>2,3</sup>:

A M **R** Y I **H** A N G A S L **F** F L A V Y I **H** I F **R** G

helix *D*<sup>2,3</sup>:

R F F S L **H** Y L L P F V I A A L V A I **H** I W A F

Maquette<sup>4</sup>:

C G G G E L W K L **H** E E L L K K **F** E E L L K L **H** E E **R** L K K L

N-terminus (at open end of Cb)

C-terminus (at template of Cb)

helix *G*<sup>1</sup>:

1 2 3 4 5 6 7 8 9 0 1 2 3 4 5 6 7 8 9 0 1 2 3 4 5 6 7  
Ac L E E L **W** K K **G** E E L A K K L Q E A L E K **G** K K L A K NH<sub>2</sub>  
|  
BrAc

helix *A*<sup>3</sup>:

W **W** I W **G** I V L A F T L V L Q I V T **G** I V L

helix *C*<sup>3</sup>:

T **W** I V **G** M V I Y L L M M G T A F M **G** Y V L

1.) Rau, H. K. & Haehnel, W. *J. Am. Chem. Soc.* (1999), **120**, 468-476.

2.) Hauska, G., Nitschke, W., Herrmann, R. G. *J. Bioenerg. Boimembr.* (1988), **20**, 211-228.

3.) Gennis, R. B., Barquera, B., Hacker, B., Van Doren, S. R., Arnaud, S., Crofts, A. R., Davidson, E., Gray, K. A., Daldal, F. *J. Bioenerg. Boimembr.* (1993), **25**, 195-209.

4.) Robertson, D. E., Farid, R. S., Moser, C. C., Urbauer, J. L., Mulholland, S. E., Pidikiti, R., Lear, J. D., Wand, A. J., DeGrado, W. F., Dutton, P. L. *Nature* (1994), **368**, 425-432.

## APPENDIX H

### Molecular mechanics force field

For molecular modeling, energy minimization and MD simulation, I used the molecular mechanics force field from the program CHARMM, in which an empirical energy function that contains energy terms for bonded and non-bonded interactions is employed. The energy function has the form:

$$E = \sum_{\text{bonds}} k_b (b - b_0)^2 + \sum_{\text{angles}} k_\theta (\theta - \theta_0)^2 + \sum_{\text{dihedrals}} k_\phi (1 - \cos(n\phi - \delta)) \\ + \sum_{\text{impropers}} k_\varphi (\varphi - \varphi_0)^2 + \sum_{i=1}^N \sum_{j>i}^N \left( 4\epsilon_{ij} \left[ \left( \frac{\sigma_{ij}}{r_{ij}} \right)^{12} - \left( \frac{\sigma_{ij}}{r_{ij}} \right)^6 \right] + \frac{q_i q_j}{4\pi\epsilon_0 r_{ij}} \right)$$

where  $k_b$ ,  $k_\theta$ ,  $k_\phi$ ,  $k_\varphi$  are the bond, bond angle, dihedral angle and improper angle force constants, respectively;  $b$ ,  $\theta$ ,  $\phi$  and  $\varphi$  are bond length, bond angle, dihedral (torsion) angle and improper angle, respectively, with the subscript zero representing the equilibrium values, dependent on the atom types involved in the particular interaction. These terms describe the bonded interactions in a macromolecule. As one can see the vibrations of the bond length, bond angle and improper angle are defined by harmonic potentials oscillating around the equilibrium value. The torsion energy term is a four-atom potential, defined by the phase factor  $\delta$  and multiplicity  $n$ . The multiplicity designates the number of minima on the potential energy surface by rotation around the bond between the two central atoms.

Non-bonded energy terms describe all interactions for atoms separated by three (the so-called 1–4 term) or more bonds. Hence, the Coulomb and Lennard-Jones 6–12 terms contribute to the external (non-bonded) interactions, where  $\epsilon_{ij}$  are the Lennard-Jones well depths and  $\sigma_{ij}$  are the distances at the Lennard-Jones minimum,  $q_i$  are the partial atomic charges,  $\epsilon_0$  is the effective dielectric constant, and  $r_{ij}$  are the distances between atom pairs  $i$  and  $j$ . While the Coulomb potential describes the electrostatic interactions, van der Waals interactions and atomic contacts are represented by the Lennard-Jones potential. The electrostatic attraction that results from opposite partial atomic charges is both stronger and acts at a longer range than the van der Waals forces. Therefore, the electrostatic interactions play a crucial role in stabilizing macromolecular conformations and govern the interactions between proteins and ligands. The parameterization of the energy function was done using experimental data and quantum-chemical ab-initio calculations for small molecules.

Beside already explained potentials, the energy function can also include energy terms to constrain certain molecular conformations. For some purposes, it is useful to fix or to restrict the changes that occur in a structure during the minimization or MD simulation. The simplest type of constraint is to rigidly fix a group of atoms in their positions by not allowing them to move at all. Alternatively, one can apply several other types of soft constraints. Thus, harmonic constraints are primarily used to avoid large displacements of atoms during the energy minimization, while still allowing the structure to relax. The harmonic constraint energy term has the form:

$$E_{\text{harmonic}}(\vec{r}) = k_r (\vec{r} - \vec{r}_{\text{fix}})^2$$

To maintain the particular structural motives, dihedral constraints can be applied on the torsion angles  $\phi$ , by using energy terms like:

$$E_{\text{dihedral}}(\phi) = k_\phi (\phi - \phi_{\text{fix}})^2$$

In the same way, bond angles ( $\theta$ ) can be harmonically constrained. NOE constraints in the energy function are originally designed to drive the molecular system to fulfill experimentally derived interproton distances. Beside that, one can use the NOE-like distance constraints to keep non-bonded atom pairs at a specific distance. They have the following form:

$$E_{\text{NOE}}(R) = \begin{cases} \frac{k_{\text{min}}}{2} (R - R_{\text{min}})^2 & \text{for } R < R_{\text{min}}, \\ 0 & \text{for } R_{\text{min}} < R < R_{\text{max}}, \\ \frac{k_{\text{max}}}{2} (R - R_{\text{max}})^2 & \text{for } R > R_{\text{max}}. \end{cases}$$

CHARMM uses this empirical energy function for energy minimization, molecular dynamics simulation and vibrational analysis. There are several minimization methods incorporated in CHARMM. I applied two of them – the steepest descent and conjugate gradient algorithm. They use the first or second derivatives of the potential energy to adjust the atomic coordinates in order to find the energy (mostly local) minimum.

The dynamic properties of macromolecules can be studied by simulating their trajectories represented by a set of atomic coordinates and velocities over a time. MD simulation is performed using a classical mechanics approach in which Newton's equations of motion for all atoms of the molecular system are numerically integrated:

$$\frac{d^2 \vec{r}_i(t)}{dt^2} = m_i^{-1} \vec{F}_i$$

where  $m_i$  and  $\vec{r}_i$  are mass and position vector of atom  $i$ . The forces  $\vec{F}_i$  acting on the atoms  $i$  are related to the derivatives of the potential energy with respect to the atomic positions ( $\vec{r}_i$ ). Thus, they are defined as the gradient of the potential energy:

$$\vec{F}_i = \frac{-\partial E(\vec{r}_1, \vec{r}_2, \dots, \vec{r}_N)}{\partial \vec{r}_i}$$

Hence, the forces determine the velocities of the atoms for a given period of time. Heating of the system is achieved by assigning random velocities to the atoms according to a Gaussian distribution for a given temperature, since the temperature is directly proportional to the mean kinetic energy of the system. Then, Newton's equations of motion are solved to determine changes in atomic coordinates and velocities as a function of time. CHARMM uses the Verlet algorithm to perform this numerical integration. Since the motions in the system (protein) are very fast, the time (integration) step in MD has to be very small. In general, the time step must be significantly smaller than the period of the fastest local motion in protein, which is typically a bond stretch involving a H-atoms (less than 10 fs). For most applications, a time step of about 1 fs is appropriate. Due to these limitations only relatively short trajectories can be simulated for large systems (up to several nano-seconds), while most of biological important processes as enzymatic reactions and protein folding occur on much larger time scales.

An alternative possibility to simulate the protein dynamics offers the Langevin-equation:

$$\frac{d^2 \vec{r}_i(t)}{dt^2} = m_i^{-1} \vec{F}_i + m_i^{-1} \vec{R}_i - \beta_i \frac{d\vec{r}_i(t)}{dt}$$

It describes stochastic dynamics, where the molecular system is coupled to a heat bath of temperature  $T$ , by random force  $\vec{R}_i$ . In addition to the conventional classical equations of motions there are two more terms, a friction term  $\beta_i d\vec{r}_i(t)/dt$ , which takes energy from the system, while the random force  $\vec{R}_i$  introduces energy into the system.

## APPENDIX I

### Modeling steps to generate atomic coordinates of the artificial cytochrome b

#### Generating initial atomic coordinates of the artificial Cb

A1. Coordinates of  $\alpha$ -helices of the  $F$  and  $G$  type, which initially have the same position and orientation, were generated with the canonical backbone torsion angles of  $-57.0^\circ$ ,  $-47.0^\circ$ , and  $180.0^\circ$  for  $\phi$ ,  $\psi$ , and  $\omega$ , respectively. Using appropriate patches, the N-termini were acetylated, C-termini were amidated for both helices and the amino-group of the C-terminal lysine of helix  $G$  was acetylated.

A2. Both helices  $F$  and  $G$  were duplicated, resulting in helices  $F_1$ ,  $F_2$  and  $G_1$ ,  $G_2$ , respectively. Subsequently, the helices were rotated and translated such that an anti-parallel four-helix bundle was formed. First, helix  $F_2$  was rotated around the helix axis by  $180^\circ$  and then translated by  $15.3 \text{ \AA}$  in a direction perpendicular to the helix axis. By this rotation operation, the hydrophobic surfaces of the helices  $F$  point towards each other. The  $C_\alpha$  atom of Phe15 is exactly in the middle of helix  $F$ . The vector  $\vec{F}$  connecting the  $C_\alpha$  atoms of the Phe15 from the two helices  $F_1$  and  $F_2$  will be needed for the following modeling steps. Still, the helices  $F_1$ ,  $G_1$  and  $G_2$  coincide. Next, helix  $G_1$  was rotated by  $90^\circ$  and helix  $G_2$  by  $-90^\circ$  around their helix axes and both are translated by  $7.65 \text{ \AA}$  along the direction of the vector  $\vec{F}$  to place them exactly between the helices  $F_1$  and  $F_2$ . With the preceding rotation operations, also the hydrophobic surfaces of the helices  $G$  point towards each other. Then, both helices  $G_1$  and  $G_2$  were rotated around the vector  $\vec{F}$  by  $180^\circ$ . By this rotation operation, the helices  $G$  became anti-parallel with respect to the helices  $F$ . After that, we needed a third axis, perpendicular to the first two axes ( $\vec{F}$ , and the helix axis) to move the helices  $G$  to their final positions. This axis was given by the vector  $\vec{G}$  connecting the  $C_\alpha$  atoms of residue Ala12 of the helices  $G_1$  and  $G_2$ . Finally, helix  $G_1$  was translated along the  $\vec{G}$  axis by  $10.0 \text{ \AA}$  in one direction and helix  $G_2$  by  $10.0 \text{ \AA}$  in the opposite direction. In the resulting four-helix bundle the helices  $G_1$  and  $G_2$ , which were in opposite corners of the bundle, were  $4.7 \text{ \AA}$  more distant than the helices  $F_1$  and  $F_2$ . This asymmetry was required to accommodate for the disk-like shape of the hemes, whose largest edge to edge extension was along the direction of the vector  $\vec{G}$ .

A3. The histidines, which were supposed to axially ligate the hemes, had to be reoriented to point pair wise to each other before the hemes could be inserted and patched to the  $\text{Ne}2$  atoms of the corresponding imidazole rings. As could be seen for instance from the helical wheel (see Fig. 5.3), the histidine residues 8 and 22 of the helix  $F$  were not exactly on top of each other. Therefore, the histidines had to be reoriented individually to guarantee that the planes of the two hemes were parallel to each other. This was achieved by setting the torsion angles  $\text{N-C}\alpha\text{-C}\beta\text{-C}\gamma$  and  $\text{C}\alpha\text{-C}\beta\text{-C}\gamma\text{-N}\delta 1$  of the four histidines to the following values: His8 of  $F_1$ :  $-141.7^\circ$  and  $73.3^\circ$ ; His22 of  $F_1$ :  $-168.6^\circ$  and  $57.6^\circ$ ; His8 of  $F_2$ :  $-137.0^\circ$  and  $45.0^\circ$ ; His22 of  $F_2$ :  $-157.0^\circ$  and  $60.0^\circ$ . The resulting  $\text{Ne}2(F_1) - \text{Ne}2(F_2)$  distances were  $4.71 \text{ \AA}$  and  $4.77 \text{ \AA}$ . The angles of the normal of the imidazole planes of the four histidines with the helix axes were  $34.9^\circ$ ,  $22.0^\circ$ ,  $30.9^\circ$ ,  $28.4^\circ$ .

A4. Now, the atomic coordinates of the two identical hemes were generated. One heme was rotated by  $180^\circ$  around its virtual bond CHB-CHD and by  $180^\circ$  around its virtual bond CHA-CHC. For a definition of the bonds see Fig. 4.1. The symmetry of the heme with respect to a possible mirror plane that includes the virtual bond CHA-CHC and is orthogonal to the heme plane is violated by substituents that bind in a different way at the pyrrole rings  $B$  and  $C$  (see Fig. 4.1). Hence, the second rotation operation led to a different relative conformation of the two hemes. This conformation of the hemes, which corresponds to the one found in the

native Cb, will be considered here for most of the investigations. However, it is not obvious, which one of the two possible heme conformations applies for the artificial Cb. Therefore, for the artificial Cb we will consider also the other non-native heme conformation, which is obtained if only the first rotation operation is applied. Finally, the two hemes were translated by 20.5 Å along the direction of the CHA-CHC bond. As a result, we obtained heme conformations where the heme planes are parallel and the PR groups of the two hemes point outward.

A5. Now the two hemes were placed in the center of the helix bundle. This was achieved by placing the two iron atoms of the hemes such that they have equal distances from each of the four helix axes. To place the two iron atoms appropriately between the Nε2 atoms of the corresponding pair of histidines, the hemes were slid jointly along the helix axes. Finally, the axial histidines were patched to the corresponding hemes.

A6. Next, we generated the coordinates of the cyclic decapeptide serving as template. It consists of a pair of anti-parallel β-strands, which are connected by two type II β-turns. We started with a linear version of the decapeptide with appropriate torsion angles of the backbone. The absolute position of the template was determined by placing three backbone atoms of residue Cys1 as follows: the nitrogen atom in the origin of the coordinate system, the C<sub>α</sub> atom on the x-axis and the C atom in the xy-plane. To form the type II β-turns with Pro-Gly, the φ, ψ and ω angles of the backbone were set to -60°, 120°, -178° for Pro and to 90°, 0°, -178° for Gly, respectively. For all other residues the values of the φ, ψ, and ω backbone angles were set to -139°, 135° and -178°, respectively. The decapeptide was cyclized using a patch that forms the peptide bond between the amino group of residue Cys1 and the carboxylate group of residue Gly10. The resulting N(Cys1)-C(Gly10) bond had a length of 3.6 Å. The ideal value of 1.35 Å for that bond will be approached later on by energy minimization.

A7. Now, we placed the cyclic decapeptide in a position appropriate for docking with the four-helix bundle. To bring the plane of the template in a perpendicular orientation with respect to the helix axes, we rotated the template by 100° around the Sγ(Cys3)-Sγ(Cys8) axis. Furthermore, the template was translated by 9.2 Å along the helix axis towards the N-terminal end of the *F* helices. With two more translation operations the sulfur atoms of all four cysteines of the template were brought in close proximity to the corresponding acetylated groups of the four helices. These translations were by 14.1 Å along N(Cys3)-N(Cys8) axis, and by 4.1 Å along N(Ala2)-N(Ala7) axis. Finally, the cyclic decapeptide was patched to the four-helix bundle by thioether bonds involving the four cysteines of the decapeptide and the acetylated N-terminal Gly1 of the helices *F* and the acetylated side chains of the C-terminal Lys27 of the helices *G*.

### Structural relaxation of atomic coordinates of the artificial Cb

The molecular structure of the artificial protein resulting from the model building has still packing problems in particular with respect to the side chains. Possible strain and van der Waals clashes of atom pairs can be removed by energy minimization with appropriately applied constraining conditions using the CHARMM22 energy function. We applied different types of constraints to stabilize the molecular structure during the various phases of the structural relaxation. Before we started the process of structural relaxation a number of constraints listed below were applied and retained until the last but one minimization step. To guarantee that the imidazole planes of the axial ligands remain orthogonal to the heme plane, we applied harmonic constraints to the following heme-imidazole torsion angles for all four histidines: C1A-NA-FE-Nε2, C1B-NB-FE-Nε2, C1C-NC-FE-Nε2, C1D-ND-FE-Nε2. For a definition of the atoms see Fig. 4.1. The values of the torsion angles were kept close to the minimum at -90° for the histidines from helix *F*<sub>1</sub> and at +90° for the histidines from helix *F*<sub>2</sub>

by using a force constant of  $200.0 \text{ kcal/mol/\AA}^2$ . These constraints enforce also that the bond angle  $\text{N}\epsilon 2(\text{His-F}_1)\text{-FE-N}\epsilon 2(\text{His-F}_2)$  remains at  $180^\circ$ . Unless otherwise stated, all other constraints applied only to the actual energy minimization step. The following steps of structural relaxation were performed:

B1. All atoms were rigidly fixed with exception of the side chain atoms of the four histidines, which were energy minimized.

B2. The conformation of the salt bridges between the PR groups of the hemes and the four arginines of the helices  $F_1$  and  $F_2$  were adjusted. For this purpose, we applied distance constraints between the O2A and O2D atoms of the heme propionates and the HH22 atoms of the corresponding arginines, Arg5(F) and Arg25(F), with parameters  $k_{\text{min}} = 150 \text{ kcal/mol/\AA}^2$ ,  $k_{\text{max}} = 200 \text{ kcal/mol/\AA}^2$ ,  $R_{\text{min}} = 1.65 \text{ \AA}$ ,  $R_{\text{max}} = 1.75 \text{ \AA}$ . All atoms but the side chain atoms of the arginines were fixed and the arginine side chains were energetically minimized.

B3. Next, we adjusted the side chain conformations of the two phenylalanines dividing the cavity of the four-helix bundle, which is hosting the two hemes in two compartments of even size. The initial distance between the  $C_\zeta$  atoms of the two phenylalanines is  $4.7 \text{ \AA}$ . To improve the position and orientation of the two phenylalanines, we applied distance constraints to the atom pairs  $H_\zeta(\text{Phe1})\text{-}C_\beta(\text{Phe2})$  and  $H_\zeta(\text{Phe2})\text{-}C_\beta(\text{Phe1})$  belonging to the two different phenylalanines (1,2) with parameters  $k_{\text{min}} = k_{\text{max}} = 200 \text{ kcal/mol/\AA}^2$  and  $R_{\text{min}} = R_{\text{max}} = 6.0 \text{ \AA}$  and energetically minimized only the side chains of the phenylalanines. In this way, the planes of the two phenylalanines are constrained to be essentially orthogonal to the helix axes.

B4. Now, we relaxed all side chains by energy minimization with the exception of all arginines, phenylalanines and cysteines, whose atoms were fixed. In this way, all side chains adopt an appropriate conformation, but arginines, phenylalanines and cysteines remain in their prepared conformation.

B5. Here we energy minimized only the side chain atoms, except the cysteines. We did not want to move these side chains, which make thioether bonds with the decapeptide, before the backbone structure of the decapeptide is relaxed.

B6. Next, we fixed all atoms of the helices and the hemes, applied dihedral angle constraints on the backbone torsion angles  $\phi$ ,  $\psi$ , and  $\omega$  of the template and performed an energy minimization. Thereby, we used a harmonic force constant of  $100.0 \text{ kcal/mol/\AA}^2$  and the before determined values of the torsion angles, to define the appropriate secondary structure of the template. These constraints were maintained until the last but one minimization step.

B7. We energetically minimized the template and the thioether bonds with the helices by fixing all atoms, except of the template and of the side chains of the residues that make the thioether bonds with the template.

B8. We fixed all atoms, except the atoms of the propionate groups of the hemes and of the arginine side chains and energetically minimized the artificial protein. With these constraints, we avoided bending the heme planes, which otherwise would occur in next minimization step, where the hemes were not constrained anymore.

B9. We energy minimized the artificial Cb by applying harmonic constraints to fix all backbone atoms at their position with a force constant decreasing in five steps from  $50.0 \text{ kcal/mol/\AA}^2$  to  $0.0 \text{ kcal/mol/\AA}^2$ . In the same way we simultaneously decreased the force constant of the dihedral angle constraints applied to the template torsion angles from  $100.0 \text{ kcal/mol/\AA}^2$  to  $0.5 \text{ kcal/mol/\AA}^2$ . The set of force constants used for the five steps of structural relaxation were:  $50.0, 5.0, 1.0, 0.2, 0.0 \text{ kcal/mol/\AA}^2$  for the backbone atoms and  $100.0, 20.0, 5.0, 5.0, 0.5 \text{ kcal/mol/\AA}^2$  for the template.

B10. Finally, we removed all constraints (also the dihedral constraints applied to histidine heme torsion angles) and energetically minimized the whole model structure now without any constraints.

## ***Curriculum vitae of the author***

### **Dragan Popović**

- 1968/10/10** born in Leskovac, Yugoslavia
- 1975–1983** primary school in Leskovac (average grade: 5.00)
- 1983–1987** high school (*Gymnasium*) in Leskovac (average grade: 5.00)
- 1987–1988** military service in Strumica
- 1988–1993** study of chemistry (Faculty of science & mathematics - *PMF*) at the University of Belgrade (audited account: Diplom-Chemist for Research and Development; average grade: 9.78)
- 1989–1993** scholar of the "*Galenika-ICN*" scholarship foundation
- 1993/11/12** Diploma Thesis at the University of Belgrade, Inorganic Chemistry Department, by Prof. Svetozar Niketić (title: *The ligand field analysis of  $N_xO_{6-x}$  chromophores*, diploma examination grade: 10)
- 1994–1998** work in the Institute for Research and Development of Pharmaceutical Company "*Zdravlje*" in Leskovac
- 1998–2001** PhD student in the Macromolecular Modeling Group of Prof. E. W. Knapp in Berlin
- 1998–2001** fellow of the *Graduiertenkolleg "Dynamik und Evolution zellulärer und makromolekularer Prozesse"* (GRK 268)
- Sept. 2001** PhD thesis: *Modeling of Conformation and Redox Potentials of Hemes and Other Cofactors in Proteins*

### **Present address:**

#### **office:**

Institut für Chemie (Kristallographie)  
 Takustraße 6  
 D-14195 Berlin  
 Germany

e-mail: popovic@chemie.fu-berlin.de  
 phone: +49-30-838-53890  
 fax: +49-30-838-53464

#### **private:**

Matterhornstraße 76  
 D-14195 Berlin  
 Germany

## Publications:

### Journal articles:

- **S. D. Zarić, D. M. Popović, E.-W. Knapp (2000).** Metal ligand aromatic cation- $\pi$  interactions in metalloproteins: Ligands coordinated to metal interact with aromatic residues. *Chem. Eur. J.* **6**, 3935-3942.
- **S. D. Zarić, D. M. Popović, E.-W. Knapp (2001).** Factors determining the orientation of axially coordinated imidazoles in heme proteins. *Biochemistry* **40**, 7914-7928.
- **D. M. Popović, S. D. Zarić, B. Rabenstein, E.-W. Knapp (2001).** Artificial cytochrome b: Computer modeling and evaluation of redox potentials. *J. Am. Chem. Soc.* **123**, 6040-6053.
- **D. M. Popović, A. Zmirić, S. D. Zarić, E.-W. Knapp (2001).** Energetics of radical transfer in DNA photolyase. (**in press in J. Am. Chem. Soc.**)
- **D. M. Popović, E.-W. Knapp (2001).** Computation of the redox potentials in the series of artificial mutant heme proteins. (**in preparation**)
- **D. Winkelmann, D. M. Popović, E.-W. Knapp (2001).** *Anacystis Nidulans* DNA photolyase: Energetics of radical transfer during the charge separation. (**in preparation**)
- **P. Voigt, D. M. Popović, E.-W. Knapp (2001).** Calculation of redox potentials of the hemes in the bacterial photosynthetic reaction center. (**in preparation**)

### Theses:

- **D. M. Popović (1993).** The Ligand Field Analysis of  $N_xO_{6-x}$  Chromophores. Diploma thesis, Inorganic Chemistry Department, University of Belgrade.
- **D. M. Popović (2001).** Modeling of Conformation and Redox Potentials of Hemes and Other Cofactors in Proteins. PhD thesis, Fachbereich Biologie/Chemie/Pharmazie – Institut für Chemie, Freie Universität Berlin.